Strain engineering in Si via closely stacked, site-controlled SiGe islands

J. J. Zhang' , N. Hrauda, H. Groiss, A. Rastelli, J. Stangl, F. Schäffler, O. G. Schmidt, and G. Bauer

Citation: Appl. Phys. Lett. **96**, 193101 (2010); doi: 10.1063/1.3425776
View online: http://dx.doi.org/10.1063/1.3425776
View Table of Contents: http://aip.scitation.org/toc/apl/96/19
Published by the American Institute of Physics

Strain engineering in Si via closely stacked, site-controlled SiGe islands

J. J. Zhang,[1,a)] N. Hrauda,[1] H. Groiss,[1] A. Rastelli,[2] J. Stangl,[1] F. Schäffler,[1] O. G. Schmidt,[2] and G. Bauer[1]
[1]*Institute of Semiconductor and Solid State Physics, University Linz, A-4040 Linz, Austria*
[2]*Institute for Integrative Nanosciences, IFW Dresden, Helmholtzstr. 20, D-01069 Dresden, Germany*

(Received 19 January 2010; accepted 3 March 2010; published online 10 May 2010)

The authors report on the fabrication and detailed structural characterization of ordered arrays of vertically stacked SiGe/Si(001) island pairs. By a proper choice of growth parameters, islands which have both large sizes and high Ge fraction are obtained in the upper layer. Finite element method calculations of the strain distribution reveal that (i) the Si spacer between a pair of islands can act as a lateral quantum dot molecule made of four nearby dots for electrons and (ii) the tensile strain in a Si cap deposited on top of the stack is significantly enhanced with respect to a single layer.
 [doi:10.1063/1.3425776]

The performance of Si-based metal-oxide-semiconductor field-effect transistors (MOSFETs) can be significantly enhanced by strain, which alters the band structure.[1–3] In n-channel MOSFETs, the electron mobility in the Si channel can be enhanced through tensile strain induced by a buried $Si_{1-x}Ge_x$ layer.[4,5] This strain depends on the Ge fraction, thickness, and width of the SiGe layer.[4,6] An alternative route is represented by Si channels above coherently strained SiGe islands.[7] The advantage of SiGe islands is that islands only induce strain locally in the Si channel and they can have a larger Ge content. Although the Ge fraction in the islands increases approximately linearly with decreasing temperature, the island width decreases quadratically.[8] Therefore, strain maximization requires a careful choice of growth parameters yielding large and relatively Ge-rich islands.

In this letter, we address this issue by fabricating site-controlled arrays of two closely stacked SiGe/Si island layers. The first layer is grown at relatively high substrate temperatures on pit-patterned Si(001) substrates to guarantee accurate position control, while the Si spacer and second Ge layer are grown at lower temperatures to obtain Ge-rich islands. We investigate the structural properties of the islands and spacer layer by combining atomic force microscopy (AFM), wet chemical etching based on solutions with different chemical selectivity, transmission electron microscopy (TEM), and x-ray diffraction (XRD). We find that the SiGe islands in the stack are partially connected and that the Ge content of the islands in the second layer is remarkably increased while the lateral island size is preserved. Finite element method (FEM) calculations show that the peculiar morphology of the Si-rich spacer between two stacked islands may be used to create four nearby quantum dots for Δ_2 electrons and that tensile strain values exceeding 1.5% may be achieved in a Si channel grown on the stack.

After *ex situ* chemical cleaning, two-dimensional pit-patterned samples with a period of 400 nm were dipped in a diluted HF solution to create a hydrogen terminated surface before loading into a solid source molecular beam epitaxy system. After Si buffer growth, 15 monolayers (MLs) Ge were deposited at a substrate temperature of 720 °C. For the double-layer sample, the first island layer was followed by the growth, at 620 °C, of 12 nm Si spacer layer and 9 ML Ge. The growth rates for Si and Ge were 1.0 and 0.05 Å/s, respectively. The SiGe islands were etched at room temperature in NHH solution [1:1 vol. (28% NH_4OH):(31% H_2O_2)], which selectively etches $Si_{1-x}Ge_x$ alloys over pure Si.[9,10] The Si spacer was etched in 10% NH_4OH at 75 °C, which selectively etches pure Si over $Si_{1-x}Ge_x$. The selectivity of such solution increases with the Ge fraction x and is more than 80:1 even for $Si_{0.9}Ge_{0.1}$ while the etching rate decreases with increasing x and is ~0.12 Å/s for $x=0.1$.[11]

Figures 1(a) and 1(b) show AFM images of samples obtained after deposition of the first and the second island layer, respectively. The first island layer consists of a uniform array of barn-shaped islands while the second one consists of dome-shaped islands.[12] The corresponding surface orientation maps (SOM)[10] are plotted in the insets. In spite of the lower growth temperature used for the second Ge layer, domes have similar lateral sizes as the barns in the first layer. Figure 1(c) shows an AFM image obtained after the SiGe islands in the top layer were removed by 48 min etching in NHH solution. After this step, no clear facets are observed (see SOM in the inset). By subsequent etching for 20 s in NH_4OH we image the buried SiGe islands [Fig. 1(d)] while the underlying Si substrate is protected by the SiGe wetting layer (WL). The comparison of AFM and TEM data (see below) indicates that the spacer is completely removed during this etching step, implying an average etching rate of more than 6.0 Å/s. This value, ~50 times larger than for $Si_{0.9}Ge_{0.1}$,[11] suggests that the spacer is made of pure Si or at most of an alloy with Ge fraction well below 0.1. The {113} and {15 3 23} facets which are typical for domes are clearly seen from the SOM [inset in Fig. 1(d)] while the steeper {111} and {20 4 23} facets present before Si overgrowth [Fig. 1(a)] have disappeared: SiGe islands have transformed from barns back to domes because of alloying during Si overgrowth.[13,14]

In order to obtain additional information on the properties of the Si spacer layer, we have replaced the NH_4OH etching step with prolonged etching (in total 800 min) in NHH solution. After relatively fast removal of the top SiGe island layer [Fig. 1(c)], also the bottom island layer is removed [Fig. 1(e)]. Since the NHH solution does not appreciably etch pure Si, Fig. 1(e) indicates that each pair of stacked SiGe islands is connected by a square region with sides parallel to the ⟨110⟩ directions and by four "legs" with in-plane projections parallel to [100] and [010] directions.

a)Electronic mail: jianjun.zhang@jku.at.

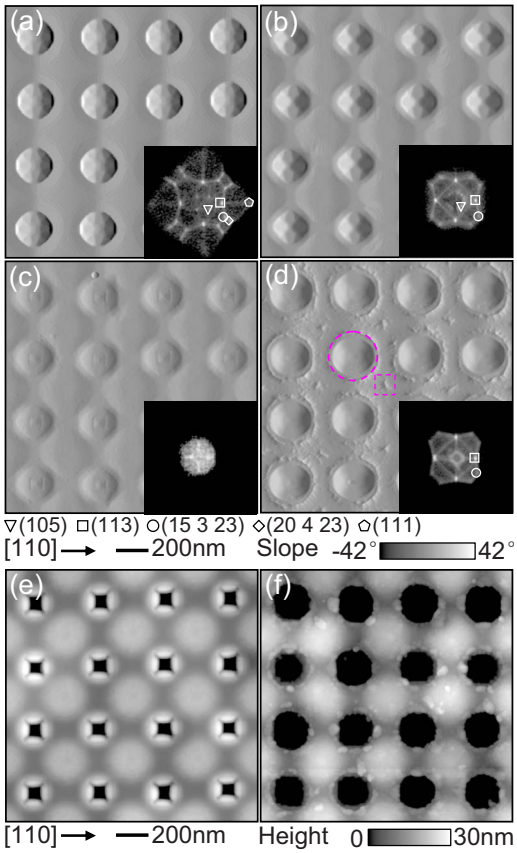

FIG. 1. (Color online) AFM images of: (a) SiGe islands obtained by depositing 15 ML Ge at 720 °C on a pit-patterned Si(001) substrate; (b) a stack with bottom SiGe layer grown as in (a) followed by 12 nm Si and 9 ML Ge at 620 °C; (c) the stack after selective removal of the top SiGe layer; and (d) after subsequent removal of the Si spacer. The insets show SOMs with different symbols marking different facets. The dashed circle and square in (d) mark regions where also the SiGe WL is removed. (e) The stack after extended SiGe etching in NHH solution and (f) after subsequent BPA etching.

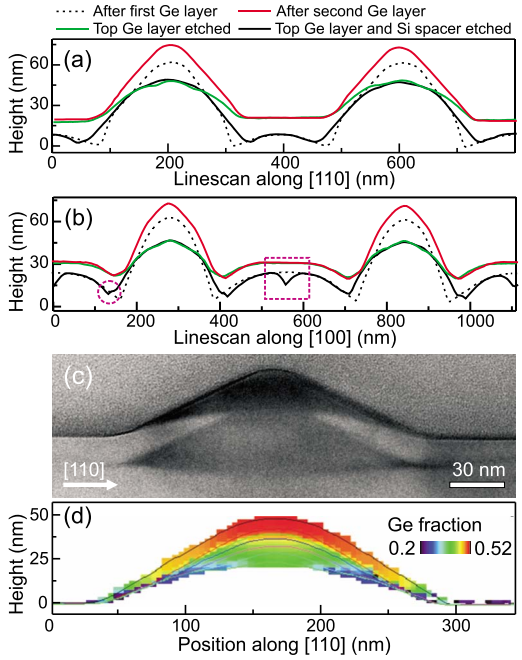

FIG. 2. (Color online) [(a) and (b)] AFM linescans passing through the island centers along [110] and [010] directions for islands shown in Figs. 1(a)–1(d), respectively. Dashed circle and square in (b) mark concave regions in the linescan, corresponding to the trench and the pit shown in Fig. 1(d). (c) Bright field cross-sectional TEM image of two closely stacked islands. (d) Cross-sectional Ge distribution along [110] direction passing through the island center obtained by selective etching in NHH solution.

The absence of a Si spacer between the apices of the bottom islands and the bases of the top islands is confirmed by the cross-sectional TEM image in Fig. 2(c). Since the etching rate of the NHH solution for SiGe decreases approximately exponentially with the Ge fraction,[9,10] Fig. 1(e) indicates that the spacer is mainly made of Si—as discussed above—but does not exclude the presence of Ge. By further etching for 2 min in a more aggressive solution [BPA, HF (1) H_2O_2 (2), CH_3COOH (3), (Ref. 15), Fig. 2(f)], also the spacer between the two islands is removed, implying that the spacer layer is not made of pure Si and that the first island layer is not fully capped with Si even after 12 nm Si overgrowth. A diluted Ge–Si alloy at the island sides can be expected due to surface-mediated intermixing and Ge segregation occurring during the capping process.[13,16]

The morphological changes at different stages of growth and etching are illustrated by AFM linescans passing through the island centers along [110] [Fig. 2(a)] and [010] [Fig. 2(b)] directions for the islands shown in Figs. 1(a)–1(d). From the linescans of the islands after the first and the second Ge layer, we see the two stacked islands are vertically aligned and the lateral size of the islands is preserved. Comparing the linescans of the first island layer before Si-overgrowth and after spacer removal, we notice a height decrease, a base width increase, and a consequent slope reduction in the side-facets, similar to previous reports [see, e.g., Refs. 13]. Interestingly, after spacer removal in NH_4OH solution, we observe small pits in the regions between nearby islands [see dashed squares in Figs. 1(d) and 2(b)] and trenches around the islands [see dashed circles in Figs. 1(d) and 2(b)]. Such features are observed also by NH_4OH etching of as-grown islands [like those in Fig. 1(a)] and indicate that the SiGe WL thickness is not homogeneous, so that thinner regions are not able to protect the underlying Si substrate during etching and appear as depressions.

Figure 2(c) shows a bright field cross-sectional TEM image of two stacked islands. Only electrons from the (000) spot were used and the sample was tilted to minimize diffraction and thus strain contrast, maximizing mass-thickness contrast, i.e., dark areas contain heavier atoms or are thicker. We clearly see that the two islands are connected, and, most importantly, that they have similar sizes but markedly different Ge content, with the top island being Ge-richer. To quantify the Ge fraction profile in the topmost islands, we employed nanotomography.[10] Figure 2(d) shows AFM linescans obtained at different stages of NHH etching and the derived Ge distribution on the (110) plane passing through the island center. The graph shows that the Ge content increases from 0.42 to 0.52 along the growth direction. The average Ge content of the top island layer is about 0.46, which is ~50% higher than the Ge fraction of islands in the first Ge layer.

Figure 3(a) shows the in-plane strain [$\varepsilon_{\parallel}=(\varepsilon_{xx}+\varepsilon_{yy})/2$] distributions on the (110) plane passing through the center of the stacked islands, as calculated by FEM with the realistic input structure. The Ge composition profiles were taken from the etching experiments for the top islands [Fig. 2(d)] and from a reference sample prior to overgrowth (Ge content increasing from 0.22 to 0.35 along the growth direction) for

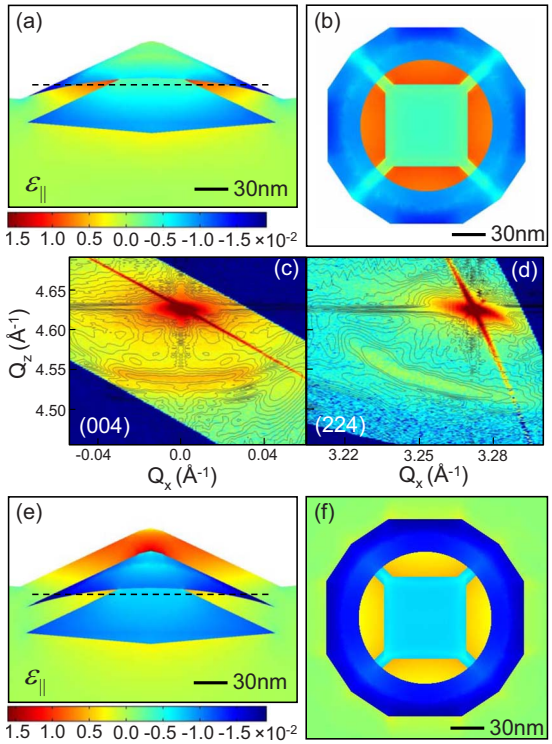

FIG. 3. (Color online) Calculated in-plane strain distributions for closely stacked islands without Si cap [(a) and (b)] and with 20 nm Si cap [(e) and (f)] on the cross-sectional (110) plane passing through island center [(a) and (e)] and on the horizontal (001) plane [(b) and (f)] at the height marked as dashed lines in [(a) and (e)]. [(c) and (d)]: experimental XRD patterns (colorplots) and calculated intensities (contours) around the (004) and (224) Bragg points, respectively.

the bottom islands. A spacer made of pure Si was assumed. In order to verify experimentally the strain fields in the ordered arrays of vertically stacked SiGe/Si(001) island pairs, diffracted x-ray intensities around the (004) and (224) Bragg points [color plots in Figs. 3(c) and 3(d)] were recorded as reciprocal space maps. These experimental data were compared to calculated diffracted x-ray intensities using kinematical diffraction theory[17] [contours in Figs. 3(c) and 3(d)]. As an input the displacement fields were taken from FEM simulations. These calculated x-ray intensities are in very good agreement with the measured XRD data, supporting the accuracy of the AFM-based structural analysis. The tensile strain in the Si spacer displays a maximum value as high as 1.22% between the top and bottom islands. The Si spacer is separated by SiGe along the [100] and [010] directions into four regions with high tensile strain, as shown in Fig. 3(b) where we plot the horizontal in-plane strain distribution at the level marked by the dashed line in Fig. 3(a). Under biaxial tensile strain, the sixfold degeneracy of the Si conduction band minimum splits into twofold degenerate Δ_2 and fourfold degenerate Δ_4 valleys.[18] The energy levels of Δ_2 are lower than those of Δ_4 and the former ones decrease linearly with tensile strain.[1,19] Thus, at low enough temperatures, the four tensile strained Si regions sandwiched between SiGe islands may act as quantum dots for electrons in the Δ_2 valleys and form a kind of lateral "quantum dot molecule."

The results shown in Figs. 1 and 2 demonstrate that stacking is a suitable route to obtain site-controlled islands which have both a rather large lateral size and a high Ge fraction. As a consequence of the increased Ge fraction, we expect that they induce a larger tensile strain in a Si cap layer compared to a single SiGe island layer. Figure 3(e) shows the in-plane strain distribution on the (110) plane passing through the center of stacked islands with 20 nm Si cap layer, covering the islands conformally, which can be realized by low temperature capping.[20] From Fig. 3(e), we see that the Si cap is tensile strained with a maximum value of 1.57%, which is a factor of 2 higher than that induced by islands only after the first Ge layer growth. As expected, the Si cap layer also leads to a reduction in the strain in the Si spacer layer, as seen by comparing the horizontal strain distributions in Figs. 3(f) and 3(b).

In conclusion, we have presented a route to obtain uniform arrays of SiGe/Si(001) islands which have both large lateral size and high Ge fraction. Strain calculations based on the experimentally determined structure show a significant enhancement of tensile strain in a Si cap grown on top of the stack. Moreover, selective wet chemical etching reveals the Si between the two closely stacked islands is separated into four tensile strained parts by SiGe, which may act as nearby quantum dots for electrons.

Work was supported by the EC d-DOTFET Project (No. 012150), the FWF (No. SFB025), the GMe Vienna, Austria, by the DFG (No. FOR730). We thank T. Fromherz for fruitful discussions.

[1] F. Schäffler, Semicond. Sci. Technol. **12**, 1515 (1997).
[2] J. L. Hoyt, H. M. Nayfeh, S. Eguchi, I. Aberg, G. Xia, T. Drake, E. A. Fitzgerald, and D. A. Antoniadis, Tech. Dig. - Int. Electron Devices Meet. **2002**, 23.
[3] M. L. Lee, E. A. Fitzgerald, M. T. Bulsara, M. T. Currie, and A. Lochtefeld, J. Appl. Phys. **97**, 011101 (2005).
[4] R. A. Donaton, D. Chidambarrao, J. Johnson, P. Chang, Y. Liu, W. K. Henson, J. Holt, X. Li, J. Li, A. Domenicucci, A. Madan, K. Rim, and C. Wann, Tech. Dig. - Int. Electron Devices Meet. **2006**, 465.
[5] K. W. Ang, C. H. Tung, N. Balasubramanian, G. S. Samudra, and Y. C. Yeo, IEEE Electron Device Lett. **28**, 609 (2007).
[6] J. G. Fiorenza, J. S. Park, and A. Lochtefeld, IEEE Trans. Electron Devices **55**, 640 (2008).
[7] O. G. Schmidt and K. Eberl, IEEE Trans. Electron Devices **48**, 1175 (2001).
[8] G. Capellini, M. De Seta, and F. Evangelisti, Appl. Phys. Lett. **78**, 303 (2001).
[9] M. Stoffel, A. Malachias T. Merdzhanova1, F. Cavallo, G. Isella, D. Chrastina, H. von Känel, A. Rastelli, and O. G. Schmidt, Semicond. Sci. Technol. **23**, 085021 (2008).
[10] A. Rastelli, M. Stoffel, A. Malachias, T. Merdzhanova, G. Katsaros, K. Kern, T. H. Metzger, and O. G. Schmidt, Nano Lett. **8**, 1404 (2008).
[11] F. Wang, Y. Shi, J. L. Liu, Y. Lu, S. L. Gu, and Y. D. Zheng, J. Electrochem. Soc. **144**, L37 (1997).
[12] J. J. Zhang, M. Stoffel, A. Rastelli, O. G. Schmidt, V. Jovanovic, L. K. Nanver, and G. Bauer, Appl. Phys. Lett. **91**, 173115 (2007).
[13] A. Rastelli, M. Kummer, and H. von Känel, Phys. Rev. Lett. **87**, 256101 (2001).
[14] M. Stoffel, A. Rastelli, J. Stangl, T. Merdzhanova, G. Bauer, and O. G. Schmidt, Phys. Rev. B **75**, 113307 (2007).
[15] T. K. Cams, M. O. Tanner, and K. L. Wang, J. Electrochem. Soc. **142**, 1260 (1995).
[16] Y. Tu and J. Tersoff (unpublished).
[17] J. Stangl, V. Holý, and G. Bauer, Rev. Mod. Phys. **76**, 725 (2004).
[18] G. Abstreiter, H. Brugger, T. Wolf, H. Jorke, and H. J. Herzog, Phys. Rev. Lett. **54**, 2441 (1985).
[19] D. Yu, Y. Zhang, and F. Liu, Phys. Rev. B **78**, 245204 (2008).
[20] N. Hrauda, J. J. Zhang, J. Stangl, A. Rehman-Khan, G. Bauer, M. Stoffel, O. G. Schmidt, V. Jovanovich, and L. K. Nanver, J. Vac. Sci. Technol. B **27**, 912 (2009).